

# Optimizing Detector Size in X-Ray Imaging

Marc Kachelrieß, *Member, IEEE*, Willi A. Kalender

*Abstract*— Image data are noisy samples acquired at discrete positions. Signal processing explicitly or implicitly involves some kind of interpolation to match a desired point spread function (PSF), to match a certain spatial resolution or to match certain contrast detection criteria. By optimization of a resolution-, noise- and dose-dependent figure of merit it was recently shown that a given spatial resolution can be best achieved using detector elements far smaller than the desired resolution element [1]. A potential dose reduction in the order of 50% was predicted when using detector elements of about half the size of the desired spatial resolution. Instead of prescribing spatial resolution we here investigate how a square wave pattern of given detail size can be best imaged in terms of contrast, noise and dose. A contrast-to-noise quality factor  $Q$  is maximized to find the optimal detector element size  $g$ .

Our findings are a potential of 70% dose reduction when using optimized flat panel detector pixel size  $g$ . This optimum lies in the order of 30% of the object detail size.

## I. INTRODUCTION

IT is common practice to push spatial resolution to the limit that is dictated by the size  $g$  of the detector elements. One reason is that detector elements smaller than absolutely necessary are said to decrease dose efficiency. This is caused by the increased ratio of total to active detector element size due to the space demanded by septa, scatter collimators, wires etc. Increased electrical component costs and increased data processing times further lead to avoiding detectors with too many channels. Data bandwidth limitations often require to reduce the number of detector pixels before read-out. Electronic combination, or binning, of neighboring detector elements is used in these cases.

Recently, we analyzed the situation in terms of spatial resolution, noise and patient dose. Our findings were that detectors of about half the size of the desired spatial resolution element are of significant advantage and allow to increase dose efficiency by a factor 1.3 (1D detector) and by a factor of 1.69 (2D detector) even in the presence of finite sized septa [1].

Our aim here is to perform a similar optimization by regarding the contrast of small structure details. We will consider a one-dimensional interpolation problem. The results can be generalized to 2D detectors by simply separating the  $x$ - and the  $y$ -direction.

## II. GENERAL CONSIDERATIONS

### A. System Model

Let  $f(x)$  be some function that we would like to assess by measuring it and let  $s(x)$  be the presampling function

Institute of Medical Physics (IMP), University of Erlangen-Nürnberg, Henkestr. 91, 91052 Erlangen. Corresponding author: Prof. Dr. Marc Kachelrieß, E-mail: marc.kachelriess@imp.uni-erlangen.de.

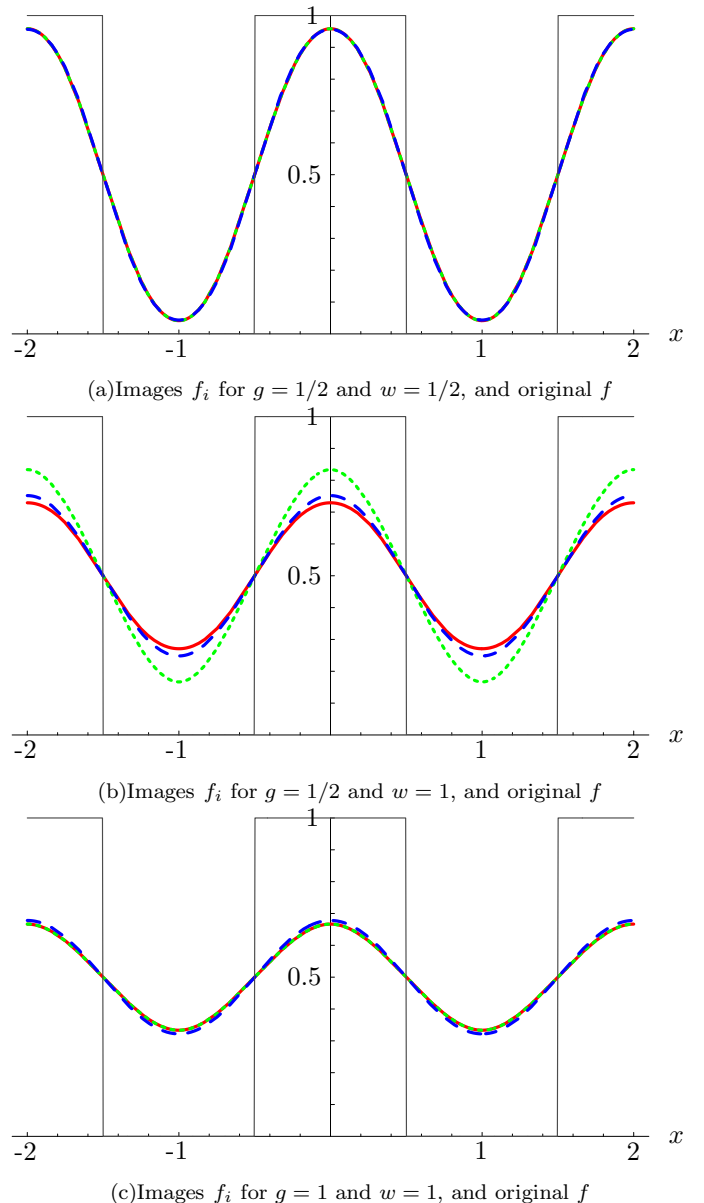
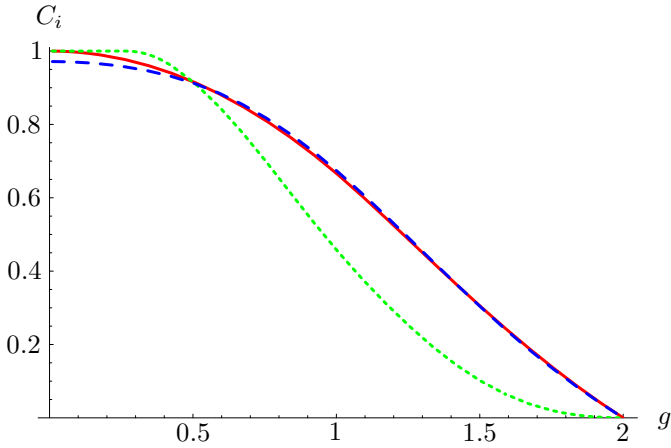
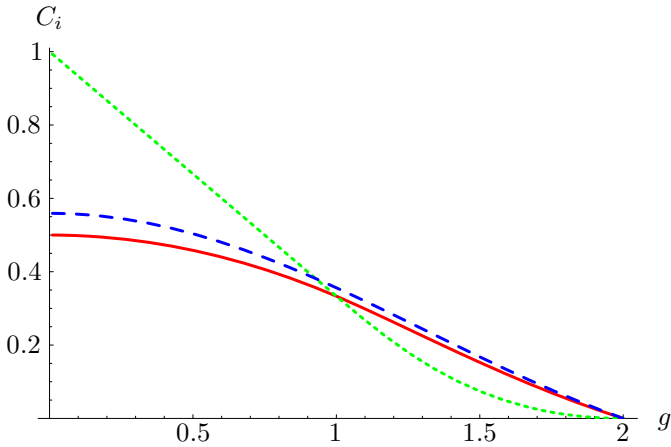


Fig. 1. Original object  $f$  (a square wave with period 2) and the resulting images  $f_i$  obtained with various  $g$  and  $w$ . The algorithms 1, 2, and 3 are color coded red, green and blue with solid, dotted and dashed style, respectively. The contrast decreases from subfigure a to subfigure c.

which comprises smoothing effects introduced by a finite sized focal spot and a finite sized integration area of the detector, for example. Its Fourier transform  $S(u)$  is the presampling MTF. The output of the detector is of the form  $f(x) * s(x)$ . This output is available, however, only at discrete sampling positions, say at spacing  $\Delta x = 1$ , and



(a) Contrast for  $w = 1/2$



(b) Contrast for  $w = 1$

Fig. 2. Contrast  $C_i$  achieved as a function of the detector size  $g$  for all three algorithms at  $w = 1/2$  and  $w = 1$ . The original object  $f$  has a contrast of 1 and a detail size of 1.

all we can assess is

$$(f(x) * s(x)) \text{III}(x),$$

with  $\text{III}(x) = \sum_n \delta(x - n)$  being the shah function.

Signal processing introduces an algorithm factor  $a(x)$  such that the final result is given by

$$\hat{f}(x) = ((f(x) * s(x)) \text{III}(x)) * a(x). \quad (1)$$

The main purpose of the algorithm factor is to provide a continuation of the discrete data samples onto  $\mathbb{R}$ . In this context we can think of  $a(x)$  being an interpolation function.

It is understood, that the presampling function and the algorithm function must be properly normalized:

$$\int dx s(x) = 1 \quad \text{and} \quad \int dx a(x) = 1.$$

To characterize  $\hat{f}(x)$  we assume that the absolute sampling position is irrelevant to the results. Our intent is to replace the shah function of equation (1) by  $\text{III}(x - t)$  and to average over all  $t$ . This is justified by the fact that the

relative orientation of our primary signal  $f(x)$  with respect to the detector pixels is random (the details that we want to visualize do not know where the sampling positions are). Mathematically, this requirement is necessary since our system, which should be linear and translation-invariant to be traceable, is only linear and translation-invariant on a scale much larger than the sampling distance. We can obtain the desired properties by averaging over  $t$  by convolving with  $\text{II}(t)$  and get

$$\bar{f}(x) = f(x) * s(x) * a(x) \quad (2)$$

and now are ready to characterize  $\bar{f}$  in place of  $\hat{f}$ . To experimentally assess the point spread function  $\text{PSF}(x) = s(x) * a(x)$  or one of its components  $s(x)$  or  $a(x)$  this averaging must be enforced by continuously varying the sampling positions, e.g. by imaging an edge or a slot that is tilted with respect to the detector axes.

From here on, sampling and the sampling distance plays no longer a role in our considerations.

### B. Noise Factor

Assuming that the detector samples are independent random variables we can determine the noise introduced (or removed) by the algorithm by error propagation. Basically, we are dealing with the filtering of noisy signals and the error propagation characteristics are well understood [2]. Let  $\sigma^2(x)$  be the variance corresponding to the value  $f(x) * s(x)$  measured at position  $x$ . Error propagation yields  $\sigma^2(x) * a^2(x)$  for the variance after signal processing. Integrating over all  $x$  gives the mean variance  $S^2 F^2$  with  $S^2 = \int dx \sigma^2(x)$  being the mean variance of the raw-data and

$$F^2 = \int dx a^2(x).$$

being the noise factor of the algorithm.

As an example assume the algorithm either to perform a nearest neighbor interpolation or to perform a linear interpolation. In the first case  $a(x) = \text{II}(x)$  and the noise variance would be multiplied by the factor 1. For the linear interpolation we have  $a(x) = \Lambda(x)$  and the factor introduced by the algorithm is  $F^2 = 2/3$ .

### C. Noise Performance at Specified MTF

A general result can be obtained by regarding the noise factor as a function of presampling  $S(u)$  for a specified system modulation transfer function  $\text{MTF}(u)$ , i.e. for specified spatial resolution and thus specified object contrast. To do so, we fix  $\text{MTF}(u) = S(u)A(u)$  where  $A(u)$  is the Fourier transform of  $a(x)$ . Rayleigh's theorem tells us that

$$F^2 = \int dx a^2(x) = \int du A^2(u) = \int du \frac{\text{MTF}^2(u)}{S^2(u)}$$

where it is assumed that the specified MTF has its cut-off before the first zero of  $S(u)$  occurs. Regarding two systems, system A with small detectors and system B with large detectors, we find that for well-behaved presampling functions the inequality  $S_A(u) \geq S_B(u)$  will hold with strict

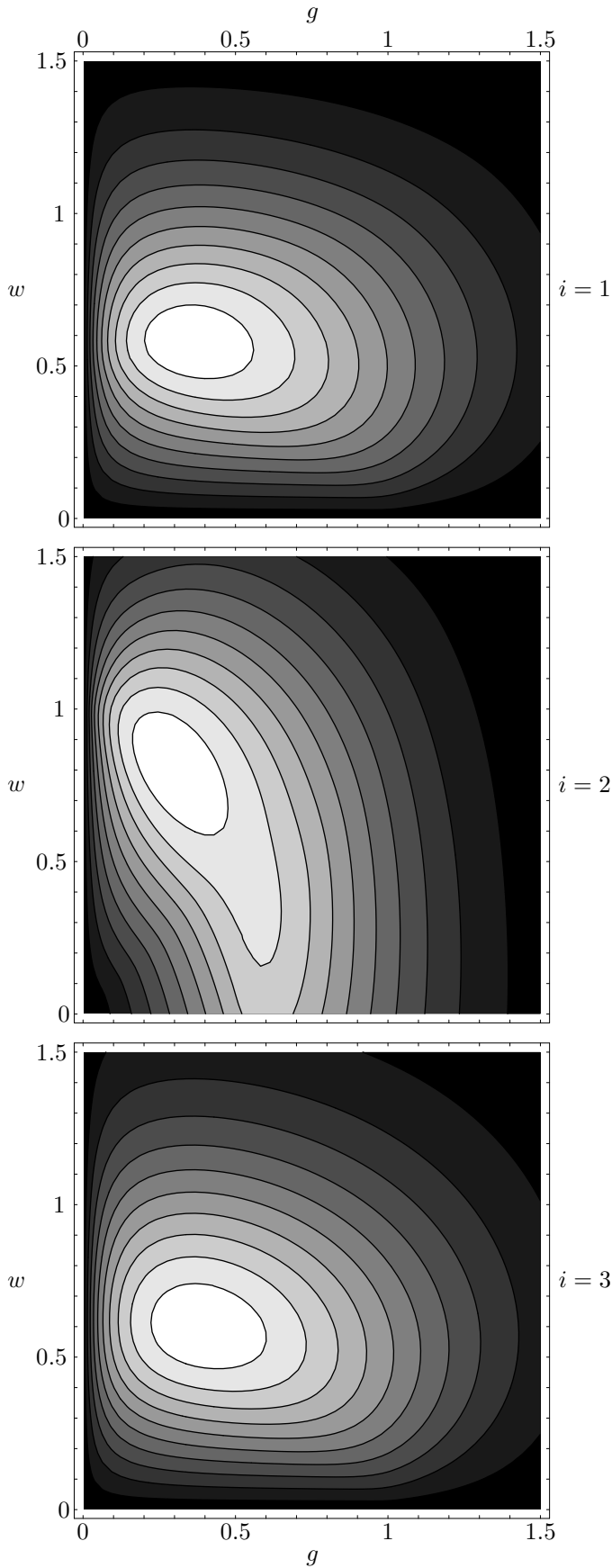


Fig. 3. For a septum size of  $\delta = 0.1$  this contour plot shows the function  $Q_i^2(w, g, \delta)$  for the three algorithms  $i = 1, 2, 3$ .

inequality almost everywhere. Consequently  $F_A^2 < F_B^2$  and system A will exhibit less image noise than system B although both systems have the same spatial resolution, contrast and dose. This implies that smaller detectors are to be preferred over larger detectors. Note that case B can also be achieved by binning detector elements of type A. Hence, binning should be avoided.

### III. IMAGING SYSTEM

To become more specific we will now continue and analyze if these findings apply to more practical algorithms that operate in spatial domain and that do not attempt to achieve a specified MTF but rather a specified contrast value  $C$ .

We assume a rectangular presampling function of width  $g$  and area 1

$$s(x) = \Pi_g^*(x) = \frac{1}{g} \Pi\left(\frac{x}{g}\right)$$

and we regard three typical interpolation algorithms that allow to a) continue the discrete samples onto  $\mathbb{R}$  and b) to balance between noise and spatial resolution:

$$\begin{aligned} a_1(x) &= \Pi_{w,w}^{**}(x) & \text{PSF}_1(x) &= \Pi_{g,w,w}^{***}(x) \\ a_2(x) &= \Pi_{g,w}^{**}(x) & \text{PSF}_2(x) &= \Pi_{g,g,w}^{***}(x) \\ a_3(x) &= \frac{1}{\sqrt{\pi/3}w} e^{-3x^2/w^2} & \text{PSF}_3(x) &= \Pi_g^*(x) * a_3(x). \end{aligned}$$

The parameter  $w$  is a width parameter and will be used to adjust for optimal contrast-to-noise ratio. The algorithms  $a_i$  and the point spread functions  $\text{PSF}_i = s * a_i$  are derived and plotted in reference [1]. The rectangle functions are recursively defined as  $\Pi_{a,b}^{**} = \Pi_a^* * \Pi_b^*$  and  $\Pi_{a,b,c}^{***} = \Pi_{a,b}^{**} * \Pi_c^*$ .

The noise factor introduced by algorithm  $i$  is given by error propagation as

$$F_i^2 = \int dx a_i^2(x).$$

Image noise is given by  $N_i^2 = F_i^2(g + \delta)/(gD)$  with  $D$  being a measure of patient dose,  $g$  being the size of the active detector element and  $\delta$  being the thickness of the septa which is assumed to be independent of  $g$ . The factor  $(g + \delta)/g$  accounts for the fact that only the fraction  $g/(g + \delta)$  of dose  $D$  contributes to the measurement. The quantities  $F_i$  and  $N_i$  are analytically derived in reference [1] for the three algorithms.

### IV. OBJECT AND CONTRAST

Let the object  $f(x) = \sum_k \Pi(x - 2k) = \Pi(x) * \text{III}(x/2)/2$  be a square wave pattern of detail size 1 (period 2) and let

$$\bar{f}_i(x) = f(x) * \text{PSF}_i(x)$$

be its image. An example of the images  $f_i$  produced using various combinations of  $g$  and  $w$  is shown in figure 1. We can clearly see that larger detector sizes  $g$  and/or larger algorithm widths  $w$  blur the image. The rectangle function is imaged less accurately and the contrast

$$C_i = \bar{f}_i(0) - \bar{f}_i(1) = 2\bar{f}_i(0) - 1,$$

defined as the difference between the minimum and the maximum values that are reproduced by the algorithms, is reduced for the smoother images.

The contrast as a function of the aperture size  $g$  is shown in figure 2 for the same two settings  $w = 1/2$  and  $w = 1$ . The full object contrast cannot be restored for the  $w = 1$  case unless very small detectors are used. For the sharper reconstruction with  $w = 1/2$  there is some region for small  $g$  where  $C_i \approx 1$  is obtained. It is interesting to note that there is still some contrast in the region  $g > 1$  where the detector is larger than the object detail to be resolved.

## V. IMAGE QUALITY

Let the (squared) contrast-to-noise ratio at unit dose (CNRD)

$$Q_i^2 = \frac{C_i^2}{N_i^2 D} = \frac{C_i^2}{F_i^2} \frac{g}{g + \delta}$$

be the underlying measure of image quality that is to be optimized. Note that  $Q_i = Q_i(w, g, \delta)$ . Figure 3 shows contour plots of  $Q_i^2$  as a function of detector size  $g$  and interpolation width  $w$  for septa of size  $\delta = 0.1$ . We can clearly see, that there is a region of optimal image quality near  $g = 0.4$ . The width  $w$  corresponding to this optimum is depending on the algorithm, of course.

For  $g$  given we define the optimum achievable image quality by tuning the algorithm parameter  $w$  as

$$Q_{\text{opt},i}^2(g, \delta) = \max_w Q_i^2(w, g, \delta).$$

The corresponding optimal detector size  $g$  and algorithm width  $w$  are given as

$$g_{\text{opt},i}(\delta) = \operatorname{argmax}_g \max_w Q_i^2(w, g, \delta)$$

$$w_{\text{opt},i}(\delta) = \operatorname{argmax}_w \max_g Q_i^2(w, g, \delta).$$

Figure 4 plots the image quality  $Q_{\text{opt},i}^2(g, \delta)$  that is achievable for a septa size of  $\delta = 0.1$ . It should be noted

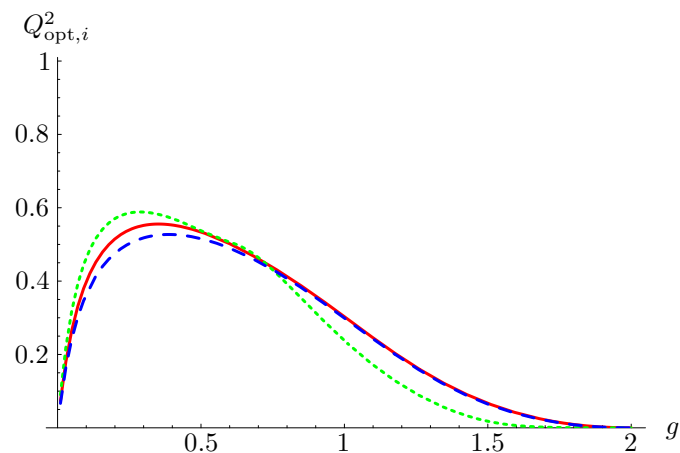


Fig. 4. The best achievable contrast for a septa size of  $\delta = 0.1$  and a given aperture size  $g$ . Here, detector sizes in the range  $g = 0.2$  to  $g = 0.4$  are of significant advantage compared to larger or smaller detectors.

that the septa size is a relative measure compared to the size of the object details to be resolved. Thus, figure 4 assumes septa of one tenth of the size of the detail. Note that considerable improvements in  $Q^2$  are achieved when using detectors that are much smaller than the details that shall be resolved. This is the case even though septa, that are a penalty to small detector sizes, are present.

Specifically,  $Q^2$  increases from about 0.30 when using large detectors with  $g = 1$  to up to 0.6 for detectors with  $g$  being in the order of 0.3. This is an increase of dose efficiency by a factor of 2.0 (1D detector) which can be used to reduce dose by  $1 - 1/2.0 = 50\%$  compared to the non-optimized case.

The differences between the three particular algorithms are rather small compared to the effect that is obtained when changing the size  $g$ .

## VI. CONVERTING TO 2D

Up to here, only one-dimensional detectors were considered. Although the conversion to multi-dimensional detectors is straightforward we will briefly show how the results convert to two-dimensional arrays such as flat-panel detectors, for example.

The noise factor in two dimensions is given by

$$F_{xy} = \int dx dy a^2(x, y) = \int dx a_x^2(x) \int dy a_y^2(y) = F_x F_y$$

where we assumed the two-dimensional algorithm  $a(x, y)$  to decompose into a product of two one-dimensional functions  $a_x(x)$  and  $a_y(y)$ . The geometrical efficiency factor  $g/(g + \delta)$  that accounts for the septa becomes

$$\frac{g_x}{g_x + \delta_x} \frac{g_y}{g_y + \delta_y}.$$

The two-dimensional analogon to the square-wave  $f(x)$  is the checkboard

$$f(x, y) = f(x)f(y) + f(x - 1)f(y - 1).$$

For the contrast we then find

$$C_{xy} = \bar{f}(0, 0) - \bar{f}(0, 1) = C_x C_y.$$

The quality figure of merit is finally given as

$$Q_{xy} = Q_x Q_y$$

and our one-dimensional results can be converted to multi-dimensional detectors by simple multiplication.

## VII. DISCUSSION

Maximizing the contrast-, dose- and noise-dependent figure of merit  $Q$  shows that detectors should be selected far smaller than the desired resolvable detail size and detector binning should be avoided. An increase of  $Q^2$  by a factor of 2.0 compared to  $g = 1$  was demonstrated under the presence of moderately sized septa (figure 4). This corresponds to a dose reduction potential of 50%. Performing

that optimization in both detector dimensions of an area detector would increase the dose usage by a factor of 4.0 and therefore yield a dose reduction of 75%. Note that similar results are obtained when optimizing with respect to a spatial resolution-based figure of merit [1]. This indicates that our findings are not specific to the figure of merit presented here but may apply for more general detection tasks.

#### REFERENCES

- [1] M. Kachelrieß and W. A. Kalender, “Presampling, algorithm factors and noise: Considerations for CT in particular and for medical imaging in general,” *Med. Phys.*, vol. 32, pp. 1321–1334, May 2005.
- [2] H. Barrett and W. Swindell, *Radiological Imaging*. Academic Press, New York, 1981.